THE 3D STRESS FIELD AT THE INTERSECTION OF A HOLE AND A FREE SURFACE IN A TRANSVERSELY ISOTROPIC PLATE

by
E. S. Folias

August 1989

University of Utah
Department of Mathematics
Salt Lake City UT 84112

Abstract

This paper deals with the analytical, 3D, stress field in the neighborhood of the intersection of a hole and the free surface of a transversely isotropic plate of $[0^o]$ orientation. The analysis shows the stresses to be proportional to $\rho^{\alpha-6}$, where the exponent α depends on the material properties of the plate as well as the polar angle θ (see fig. 1). For the special case of a graphite/epoxy plate the value of α, at the critical location $\theta = 0$, is shown to be $\alpha = 5.573$ which implies a rather strong stress singularity. Finally, the physical meaning of these results to the process of fatigue damage are discusssed and compared with existing experimental observations.

1 Introduction

It is well known that at the vertex of a sector plate, both in bending and stretching, unbounded stresses may occur for certain vertex angles. In the case of a homogeneous and isotropic materials this matter has been investigated analytically, subject to various edge conditions and based on 2D consideration, by Williams (1951, 1952). To the best of the author's knowledge an explicit analytical solution for the determination of the 3D stress field in the neighborhood of the corner point has yet to be constructed. A somewhat complete historical update of the subject can be found in references (Cruse 1988, Rosakis et. al 1989).

On the other hand, for the simpler case of a thick homogeneous and isotropic plate that has been weakened by the presence of a circular hole, Folias (1987) was able to extract, analytically, the explicit 3D stress field in the vicinity where the hole meets the free surface of the plate. The analysis shows that the stress field there is non–singular. In the present paper, the author extends his analysis to also include transversely isotropic plates. As a practical matter, it is hoped that the solution will evince many characteristics of the stress field at such neighborhoods and that it will provide guidance for the proper undestanding of the phonomenon of fatigue damage in laminated composite structures, where drilling and bolting still remains to be a common method of joining.

2 Formulation of the Problem

Consider the equilibrium of a homogeneous, transverely isotropic, elastic plate that occupies the space $|x| < \infty$, $|y| < \infty$, $|z| \leq h$ and contains a cylindrical hole of radius a whose generators are perpendicular to the bounding planes, namely $z = \pm h$. Let the plate be subjected to a uniform tensile load σ_0 along the y–axis and parallel to the bounding planes (see Fig. 1).

In the absence of body forces, the coupled differential equations governing the displacement functions u, v, and w are

$$C_{11}\frac{\partial^2 u}{\partial x^2} + C_{66}\frac{\partial^2 u}{\partial y^2} + C_{55}\frac{\partial^2 u}{\partial z^2} + (C_{12}+C_{66})\frac{\partial^2 v}{\partial x \partial y} + (C_{13}+C_{55})\frac{\partial^2 w}{\partial x \partial z} = 0 \tag{1}$$

$$(C_{21}+C_{66})\frac{\partial^2 u}{\partial x \partial y} + C_{66}\frac{\partial^2 v}{\partial x^2} + C_{22}\frac{\partial^2 v}{\partial y^2} + C_{44}\frac{\partial^2 v}{\partial z^2} + (C_{23}+C_{44})\frac{\partial^2 w}{\partial y \partial z} = 0 \tag{2}$$

$$(C_{31}+C_{55})\frac{\partial^2 u}{\partial x \partial z} + (C_{32}+C_{44})\frac{\partial^2 v}{\partial x \partial z} + C_{55}\frac{\partial^2 w}{\partial x^2} + C_{44}\frac{\partial^2 w}{\partial y^2} + C_{33}\frac{\partial^2 x}{\partial z^2} = 0 \tag{3}$$

where the C_{ij}'s are the material constants defining a layer which has its fibers running parallel to the x–axis.

The stress–displacement relations for the layer are given by the constitutive relations

$$\begin{bmatrix} \sigma_{xx} \\ \sigma_{yy} \\ \sigma_{zz} \\ \tau_{yz} \\ \tau_{xz} \\ \tau_{xy} \end{bmatrix} = \begin{bmatrix} C_{11} & C_{12} & C_{13} & 0 & 0 & 0 \\ C_{21} & C_{22} & C_{23} & 0 & 0 & 0 \\ C_{31} & C_{32} & C_{33} & 0 & 0 & 0 \\ 0 & 0 & 0 & C_{44} & 0 & 0 \\ 0 & 0 & 0 & 0 & C_{55} & 0 \\ 0 & 0 & 0 & 0 & 0 & C_{66} \end{bmatrix} \begin{bmatrix} e_{xx} \\ e_{yy} \\ e_{zz} \\ 2e_{yz} \\ 2e_{xz} \\ 2e_{xy} \end{bmatrix} \tag{4}$$

As to boundary conditions, we require that:

at $z = \pm h:$ the surface stresses must vanish (5)

at $r = a:$ the surface stresses must vanish. (6)

Finally, in order to complete the formulation of the problem, the loading conditions far away from the hole must be satisfied.

3 Method of Solution

The main objective of this investigation is to construct an asymptotic solution which is valid in the immediate vicinity of the corner point, i.e. the neighborhood where the hole surface intersects the plate surface $z = h$. Guided by a general analytical solution to the equilibrium of transversely isotopic layers which the author has recently constructed (Folias 1988), we assume the complementary displacement field in the form

$$u = \sin\theta \left\{ \ell_{11} \frac{\partial^2}{\partial (r-a)^2} + \ell_{12} \frac{\partial^2}{\partial (h-z)^2} \right\} \frac{\partial^3 H}{\partial (r-a) \partial (h-z)^2} \tag{7}$$

$$v = \cos\theta \left\{ \ell_{21} \frac{\partial^2}{\partial (r-a)^2} + \ell_{22} \frac{\partial^2}{\partial (h-z)^2} \right\} \frac{\partial^3 H}{\partial (r-a) \partial (h-z)^2} \tag{8}$$

$$w = \left\{ \ell_{31} \frac{\partial^4}{\partial (r-a)^4} + \ell_{32} \frac{\partial^4}{\partial (r-a)^2 \partial (h-z)^2} + \ell_{33} \frac{\partial^4}{\partial (h-z)^4} \right\} H \tag{9}$$

where

$$\ell_{11} = -(C_{13} + C_{55}) \left[C_{66} \sin^2\theta + C_{22} \cos^2\theta \right] + (C_{12} + C_{66})(C_{23} + C_{44}) \cos^2\theta \tag{10}$$

$$\ell_{12} = -(C_{13} + C_{55}) C_{44} \tag{11}$$

$$\ell_{21} = (C_{13} + C_{55})(C_{21} + C_{66}) \sin^2\theta - (C_{23} + C_{44})(C_{11} \sin^2\theta + C_{66} \cos^2\theta) \tag{12}$$

$$\ell_{22} = -(C_{23} + C_{44}) C_{55} \tag{13}$$

$$\ell_{31} = (C_{11} \sin^2\theta + C_{66} \cos^2\theta)(C_{66} \sin^2\theta + C_{22} \cos^2\theta) - \frac{1}{4}(C_{12} + C_{66})^2 \sin^2(2\theta) \tag{14}$$

$$\ell_{32} = C_{44}(C_{11} \sin^2\theta + C_{66} \cos^2\theta) + C_{55}(C_{66} \sin^2\theta + C_{22} \cos^2\theta) \tag{15}$$

$$\ell_{33} = C_{44}C_{55}. \tag{16}$$

In writing the above displacements, we used a cylindrical coordinate system and, furthermore, assumed that $(r-a) << a$. In view of the above, one can show that the unknown function H must now satisfy the differential relation

$$\left[\frac{\partial^2}{\partial(r-a)^2} + \epsilon_1 \frac{\partial^2}{\partial(h-z)^2}\right]\left[\frac{\partial^2}{\partial(r-a)^2} + \epsilon_2 \frac{\partial^2}{\partial(h-z)^2}\right] \cdot \cdot \left[\frac{\partial^2}{\partial(r-a)^2} + \epsilon_3 \frac{\partial^2}{\partial(h-z)^2}\right] H = 0, \tag{17}$$

where the ϵ_1, ϵ_2 and ϵ_3 are functions of C_{ij} and θ and represent the roots of the cubic equation

$$\epsilon^3 - \frac{T_2}{T_1}\epsilon^2 + \frac{T_3}{T_1}\epsilon - \frac{T_4}{T_1} = 0, \tag{18}$$

with

$$\begin{aligned} T_1 &= (C_{11}\sin^2\theta + C_{66}\cos^2\theta)(C_{66}\sin^2\theta + C_{22}\cos^2\theta)(C_{55}\sin^2\theta + C_{44}\cos^2\theta) \\ &-\frac{1}{4}(C_{12}+C_{66})^2(C_{55}\sin^2\theta + C_{44}\cos^2\theta)\sin^2(2\theta) \end{aligned} \tag{19}$$

$$\begin{aligned} T_2 &= (C_{11}\sin^2\theta + C_{66}\cos^2\theta)\Big[C_{33}(C_{66}\sin^2\theta + C_{22}\cos^2\theta) + \\ &+ C_{44}(C_{55}\sin^2\theta + C_{44}\cos^2\theta) - (C_{23}+C_{44})^2\cos^2\theta\Big] \\ &+(C_{12}+C_{66})\Big[2(C_{23}+C_{44})(C_{31}+C_{55})\sin^2\theta - (C_{21}+C_{66})C_{33}\sin^2\theta\Big]\cos^2\theta \\ &-(C_{13}+C_{55})^2(C_{66}\sin^2\theta + C_{22}\cos^2\theta)\sin^2\theta \\ &+C_{55}(C_{66}\sin^2\theta + C_{22}\cos^2\theta)(C_{55}\sin^2\theta + C_{44}\cos^2\theta) \end{aligned} \tag{20}$$

$$T_3 = C_{55}\Big[C_{33}(C_{66}\sin^2\theta + C_{22}\cos^2\theta) + C_{44}(C_{55}\sin^2\theta + C_{44}\cos^2\theta)$$

$$- (C_{23} + C_{44})^2\cos^2\theta\Big] - (C_{13} + C_{55})^2 C_{44}\sin^2\theta$$

$$+ \Big[C_{11}\sin^2\theta + C_{66}\cos^2\theta\Big] C_{33}C_{44} \tag{21}$$

$$T_4 = C_{33}C_{44}C_{55}. \tag{22}$$

It remains, therefore, for us to construct a solution to equation (17). To accomplish this, we introduce the local, to the corner, stretched coordinate system (see Fig. 2), i.e.

$$r - a = \rho\cos\phi \tag{23}$$

$$\frac{(h-z)}{\epsilon_1} = \rho\sin\phi. \tag{24}$$

Omitting the long and tedious mathemataical details, the solution to equation (17), in terms of the local coordinates, is found to be

$$H(\rho,\phi) = \rho^\alpha\left\{A_1\cos(\alpha\phi) + B_1\sin(\alpha\phi) + \frac{1}{\alpha}\int_0^\phi \psi_1(\xi)\sin\left[\alpha(\phi-\xi)\right]d\xi\right], \tag{25}$$

where

$$\psi_1(\phi) = \{A_2\cos\left[(\alpha-2)\phi_2\right] + B_2\sin\left[(\alpha-2)\tan^{-1}(\phi_2)\right]$$

$$+\frac{1}{(\alpha-2)}\int_0^{\phi_2}\psi_2(\xi)\sin\left[(\alpha-2)(\phi_2-\xi)\right]d\xi\ \}\left(\frac{\rho_2}{\rho}\right)^{\alpha-2}, \tag{26}$$

$$\frac{\rho_2}{\rho} = \frac{\sqrt{1+\frac{\epsilon_1}{\epsilon_2}\tan^2\phi}}{\sqrt{1+\tan^2\phi}}, \tag{27}$$

$$\psi_2(\phi_2) = \left(\frac{\rho_3}{\rho_2}\right)^{\alpha-4} \quad \{ A_3 \cos\left[(\alpha-4)\tan^{-1}\left(\sqrt{\frac{\epsilon_2}{\epsilon_3}}\tan\phi_2\right)\right]$$

$$+B_3 \sin\left[(\alpha-4)\tan^{-1}\left(\sqrt{\frac{\epsilon_2}{\epsilon_3}}\tan\phi_2\right)\right] \}, \tag{28}$$

$$\left(\frac{\rho_3}{\rho_2}\right) = \sqrt{\frac{1+\frac{\epsilon_2}{\epsilon_3}\tan^2\phi_2}{1+\tan^2\phi_2}} \tag{29}$$

$$\phi_2 = \tan^{-1}\left(\sqrt{\frac{\epsilon_1}{\epsilon_2}}\tan\phi\right), \tag{30}$$

and α, A_i and $B_i(i = 1,2,3)$ are constants to be determined from the boundary conditions, i.e. the stresses along the surfaces $\phi = 0$ and $\phi = \pi/2$ must vanish for all ρ. More specifically,

$$\sigma_{zz}(\rho, 0) = 0 \tag{31}$$

$$\tau_{xz}(\rho, 0) = 0 \tag{32}$$

$$\tau_{yz}(\rho, 0) = 0 \tag{33}$$

$$\sigma_{rr}\left(\rho, \frac{\pi}{2}\right) = 0 \tag{34}$$

$$\tau_{r\theta}\left(\rho, \frac{\pi}{2}\right) = 0 \tag{35}$$

$$\tau_{rz}\left(\rho, \frac{\pi}{2}\right) = 0. \tag{36}$$

Without going into the mathematical details, the above equations lead to a system of six algebraic equations, the determinant of which must vanish. This latter condition leads to the determination of the characteristic values α. In gneral, the values of α depend on the material constants C_{ij}, as well as on the angle θ. As a practical matter, if one considers the case of a graphite/epoxy layer, with coefficients C_{ij} (Knight 1982)

$$C_{ij} = \begin{bmatrix} 20.6228 & 1.0381 & 1.0381 & 0.0000 & 0.0000 & 0.0000 \\ 1.0381 & 2.2301 & 1.2301 & 0.0000 & 0.0000 & 0.0000 \\ 1.0381 & 1.2301 & 2.2301 & 0.0000 & 0.0000 & 0.0000 \\ 0.0000 & 0.0000 & 0.0000 & 0.5000 & 0.0000 & 0.0000 \\ 0.0000 & 0.0000 & 0.0000 & 0.0000 & 0.8696 & 0.0000 \\ 0.0000 & 0.0000 & 0.0000 & 0.0000 & 0.0000 & 0.8696 \end{bmatrix} \qquad (37)$$

then the requirement of the determinant of the system (31)–(36) to vanish leads to a transcendental equation for the roots α. The only roots of practical interest are those which lie in the interval $5 < Re\ \alpha < 6$. The numerical results for the 6×6 system were carried out in double precision. For angles of $\theta > 1^0$ there exist no real or complex roots in the above interval of interest. The quantity $(\alpha - 5)$ is a factor of the system, so $\alpha = 5$ is definately a root for all θ. The value of $\alpha = 6$ is also a root[1] for all θ greater than approximately 1^o. For smaller θ, the value of α deeps rather abruptly until it finally reaches the value of $\alpha = 5.544$. It may be noted, however, that at the same time the 6×6 system becomes ill conditioned, for at $\theta = 0$ two of the boundary conditions are automatically satisfied. Consequently, a separate analysis was carried out at this location which led to a 4×4 system the numerical solution of which gave $\alpha = 5.567$. A comparison with the value obtained from the 6×6 system shows only a 1% difference.

Thus $\alpha = 6$ is a root for all angles θ except for a very narrow band about the line $\theta = 0$ where it deeps rather abruptly until it finally reaches its lowest value[2] of $\alpha = 5.567$, while one may certainly recover the continuous spectrum of α in this narrow band by carrying out an asymptotic analysis for small θ, the author believes that such further information is of very little practical value and as a result the effort required is unjustifiable.

Perhaps it is appropriate at this point to note that if the material properties C_{ij} are altered, the band width in θ changes too. Finally, in the limit as one lets the plate become isotropic the results reported by Folias (1987) are recovered. In this case α is independent of θ and the stress field is nonsingular throughout.

[1]Note $(\alpha - 6)$ is not a factor of the sytem.

[2]A mathematical function exhibiting such a property is the probability integral.

Discussion of the results

The foregoing analysis shows that the stress field in the neighborhood of the corner points, i.e. the points where the hole surface intersects with the free of stress boundary plane, may be singular. For example, in the case of a graphite/epoxy layer defined by equation (37), the stresses are shown to be singular only in the very immediate vicinity of $\theta = 0$. More specifically, the stresses at $\theta = 0$ are shown to be proportional to $\rho^{-0.433}$. This is not totally unexpected for at this location the fibers of the layer are tangent to the hole surface. In general, the exponent α is a function of the position angle θ and of the material properties C_{ij}.

As a practical matter, the results suggest that, in the presence of a cyclic load, a small crack is most likely to manifest itself along the fiber/matrix interface BAB (see Fig. 3) . In general, the length of the advancing crack will depend on the number of cycles, the position relative to the local geometry of the hole, as well as the local to the crack applied load.[3] Moreover, the crack is also expected to advance itself towards the center of the plate. To see this, consider the case of an isotropic plate. For this case, Folias et. al. (1986) have shown that the displacement w, at this location, is negative (see Fig. 4) suggesting, therefore, that the material is pulled towards the center of the plate. Similar trends are expected to prevail in this case too. However, because the fibers are considerably stiffer than the matrix, the displacement w of the last legament of the matrix will be greater than that of the fiber and as a result the crack will also propagate in the vertical direction. More specifically, the imaginary line ACD will deform to the curve $A'C'D$, thus forming a shear crack of a very small depth AA' which decreases as one approaches the points B. Experimental evidence carried out by Bakis et. al. (1986) on fatigue failure of laminated composite plates weakened by a hole clearly shows the presence of such a crack which is tangent to the hole.

A closer inspection of the experimental evidence also shows the presence of interfacial cracks between fibers and matrix at other θ–locations. However, these are secondary cracks for their length is only of a few orders of magnitude of the fiber diameter. Such cracks are to be expected for, in view of some recent results reported by Folias (1989), the stress field in the

[3] This matter is presently under investigation.

neighborhood of the intersection of a fiber and a free surface, e.g. a hole, is singular with a much weaker stress singularity. Also, for these cracks to advance, the local to the crack applied stress must be greater than a certain nominal stress value.

For example, such cracks will be of great concern particularly in the immediate vicinity of an interface, e.g. $[0^o/45^o]$, and at certain θ–locations.

The above method of analysis may now be used successfully to investigate the interlaminar stresses in composite laminates. The results for a stacking sequence of $0^o/45^o/90^o \cdots$ laminae have recently been completed and will be reported in a subsequent paper. The results compare favorably with existing experimental observations as well as finite element analyses.

Finally, it may be noted that the results at $\theta = 0$ also shed some light on the problem of a matrix crack approaching a fiber, perpendicularly (see Fig. 5). In practice, the tip of the crack has some finite radius. Thus the local geometry at point A is similar to that of the present work and the stress field can be approximated by

$$\sigma_{ij} \sim \rho^{-0.433} f_{ij}(C_{k\ell}, \phi). \tag{38}$$

Aknowledgement

This work was supported in part by the Air Force Office of Scientific Research Grant No. AF0SR-87-0204. The author wishes to thank Lt. Col. G. Haritos for this support.

References

1. Bakis, C. E. and Stinchcomb, W. W., 1986, Response of thick, notched laminates subjected to tension–compression cyclic loads, ASTM STP 907, pp. 314-334.

2. Cruse, T. a., 1988, editor, Fracture Machanics, ASTM STP 969.

3. Folias, E. S. and Wang, J.J. 1986, "On the Three–Dimensional Stress Field Around a Circular Hole in a Plate of Arbitrary Thickness" UTEC Report, University of Utah.

4. Folias, E. S., 1987, International Journal of Fracture Vol. 35, pp. 187–194.

5. Folias, E. S., 1988, University of Utah Technical Report.

6. Folias, E. S., 1989, International Journal of Fracture, Vol. 39, pp. 25–34.

7. Rosakis, A. J. Ravi–Chandar, K., Rajapakse, Y., 1989, editors, Analytical, Numerical, and Experimental Aspects of Three dimensional Fracture Processes, ASME AMD, Vol. 91.

8. Williams, M.L., 1951, U. S. National Congress of Applied Mechanics, Illinois Institute of Technology, Chicago, IL.

9. Williams, M. L., 1952, Journal of Applied Mechanics, 19, 526–528.

Figure Captions

Fig. 1. Geometrical and loading Configuration.

Fig. 2. Definition of local coordinates at the corner.

Fig. 3. Geometrical confirguration at microscale level.

Fig. 4. Vertical displacement at the surface vs (r/a).

Fig. 5. Local geometry of a matrix notch approaching a fiber.

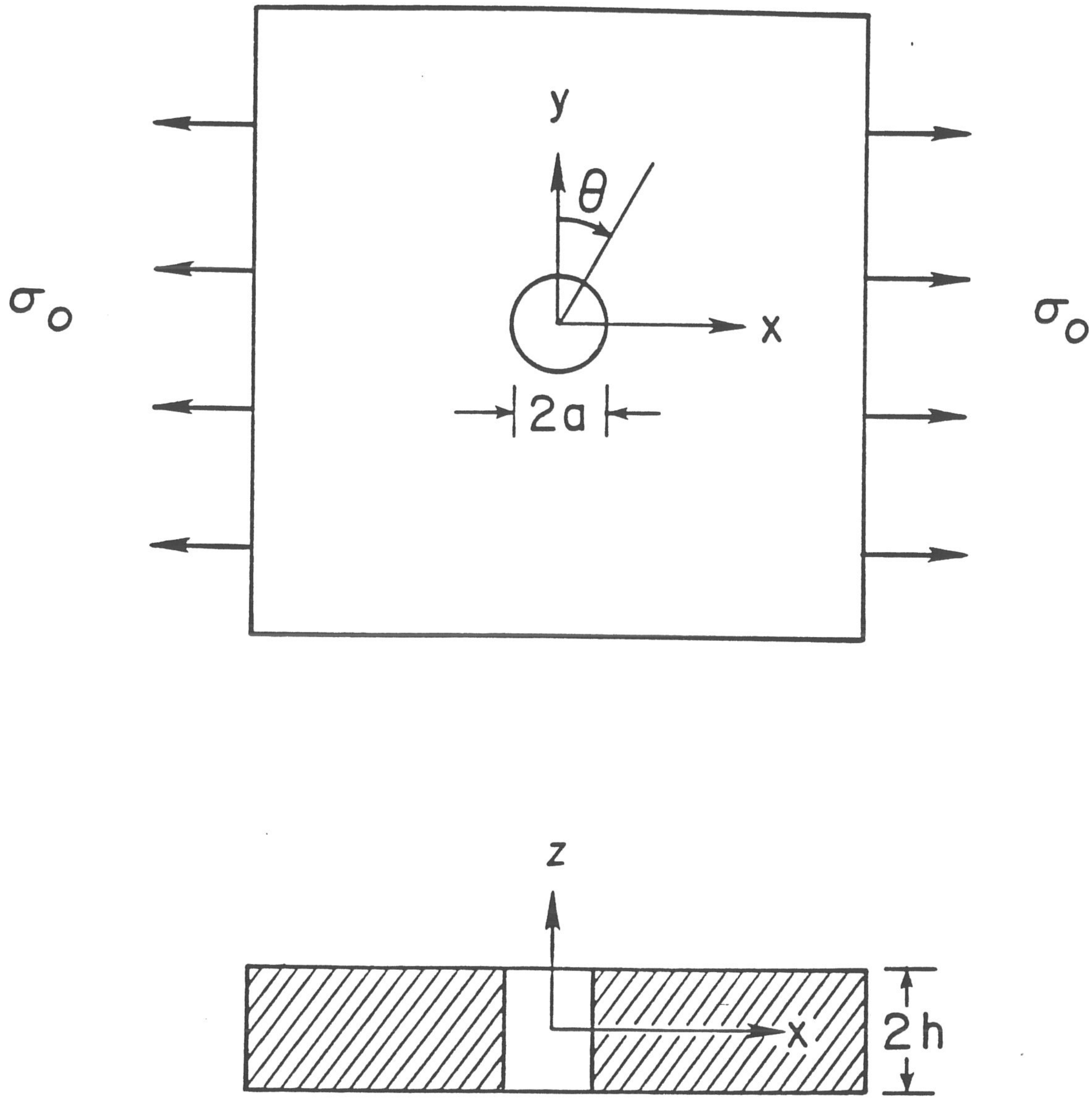

y
θ
σo
σo
x
2a
z
x
2h

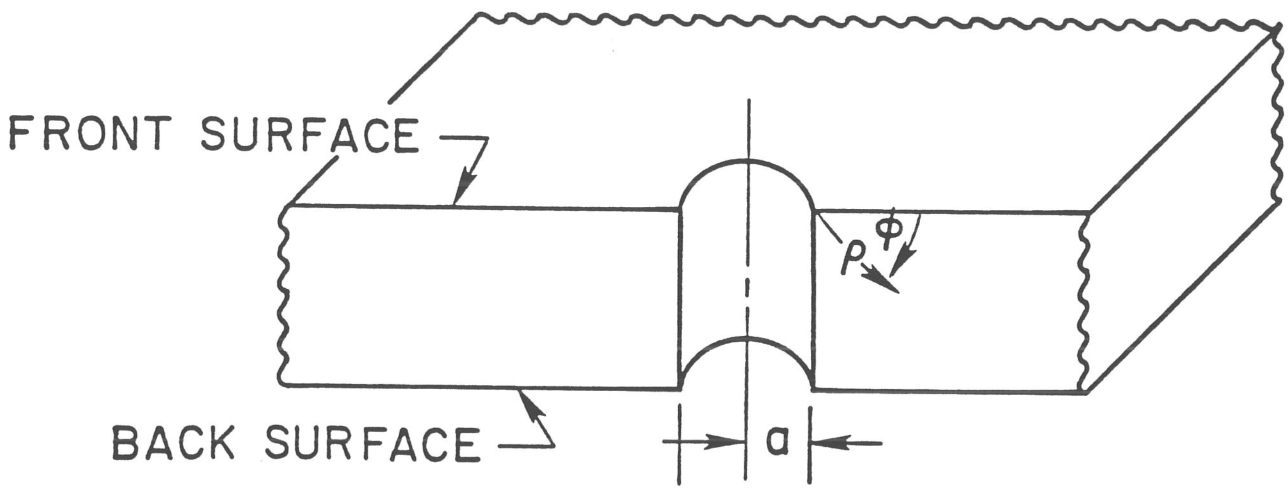
FRONT SURFACE
BACK SURFACE
ρ
φ
a

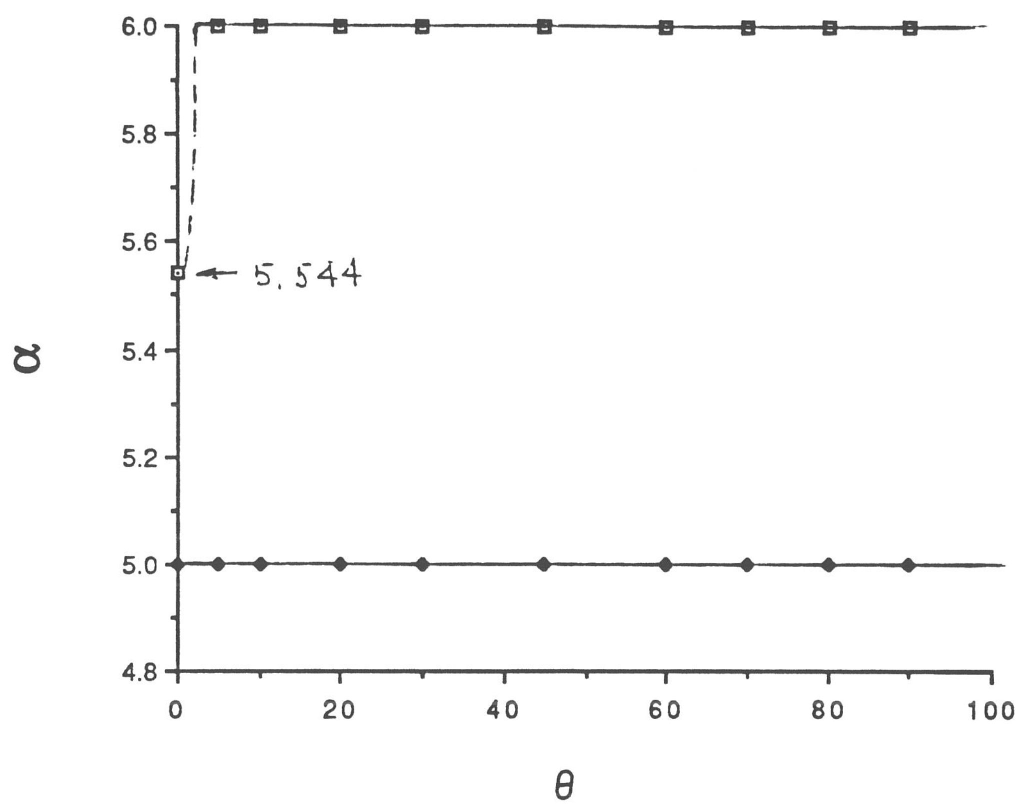

6.0
5.8
5.6
5.4
5.2
5.0
4.8
5.544
α
0
20
40
60
80
100
θ

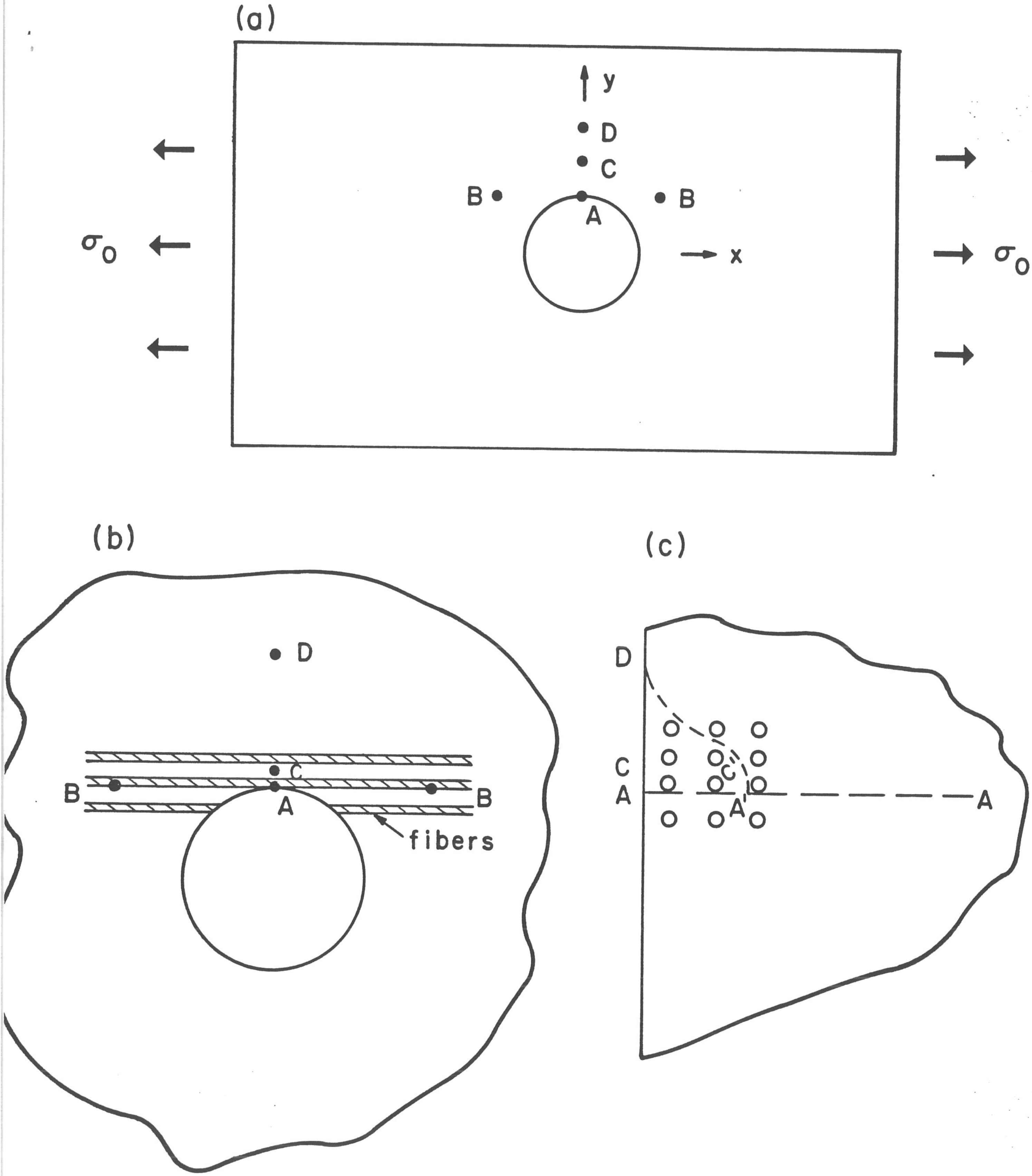

(a)
y
D
C
B
A
B
σo
x
σo
(b)
D
C
B
A
B
fibers
(c)
D
C
A
C'
A'
A

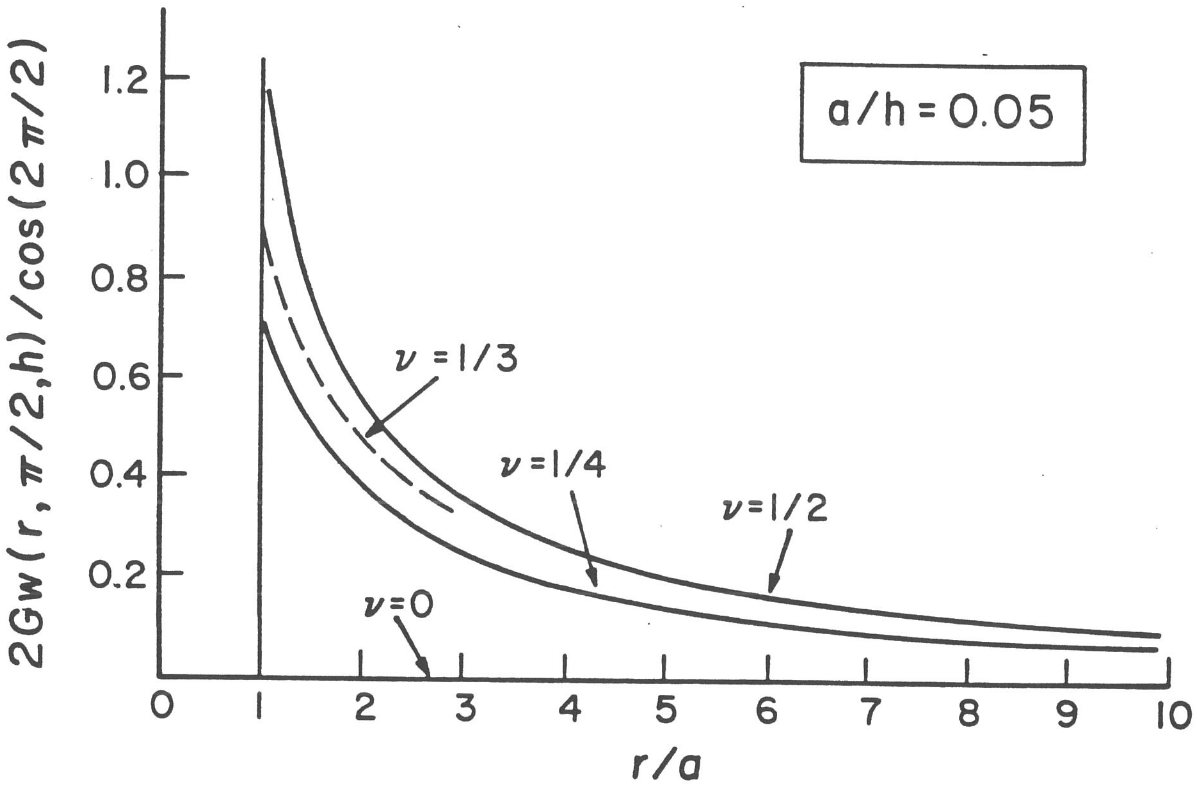

a/h = 0.05
2Gw(r, π/2, h)/cos(2π/2)
1.2
1.0
0.8
0.6
0.4
0.2
ν = 1/3
ν = 1/4
ν = 1/2
ν = 0
0
1
2
3
4
5
6
7
8
9
10
r/a

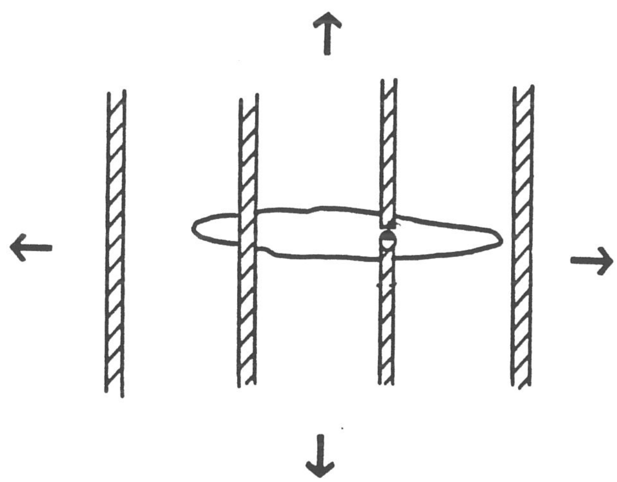

(a)

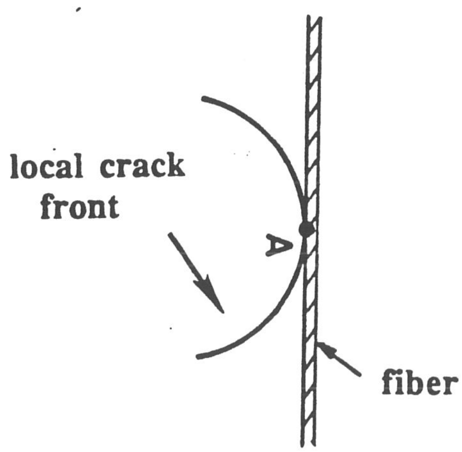

(b)

EXPERIMENTS SUPPORT EXISTENCE OF CRACK

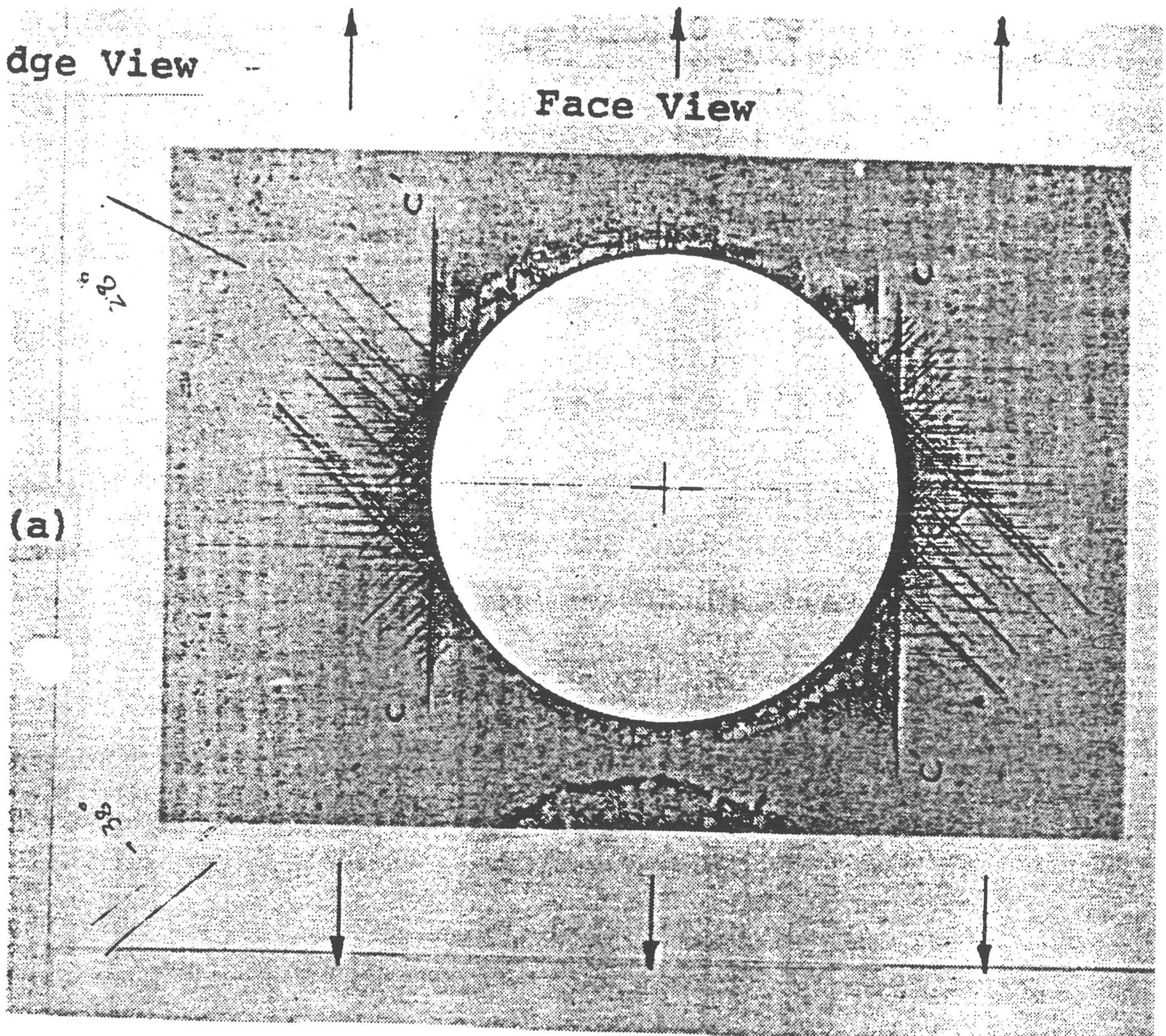

5 K cycles